



## TEN GHz SURFACE RESISTANCE OF SUPERCONDUCTING SAMPLES MEASURED BY THE DIELECTRIC RESONATOR METHOD

N. SPARVIERI\*, M. BOUTET†, B. CAMAROTA† and F. ARCIDIACONO†

\*Alenia, Research Department, Via Tiburtina Km. 12,400 00131, Rome, Italy

†CINS c/o Alenia, Research Department, Via Tiburtina Km. 12,400 00131, Rome, Italy

(Received 8 January 1997)

**Abstract**—We have set up an easy and reliable experimental apparatus to perform the surface resistance measurement at 10 GHz in the  $TE_{011}$  mode by the dielectric resonator method. This resonant system is unaffected by the measured sample shape, provided that the minimum circle inscribed in it is 10 mm; moreover any previous calibration on a standard sample is not necessary. YBCO thin films on  $LaAlO_3$ , with thickness ranging between 1000 and 6000 Å, and sintered pellets have been measured as a function of the temperature for an input power ranging between -5 and 20 dBm. © 1997 Elsevier Science Ltd.

### 1. INTRODUCTION

The discovery of High Temperature Superconductors (HTSC) has generated a great deal of interest in both basic and applied research [1-4]. Actually highly oriented thin films are the only chance to get large homogeneous surfaces for integrated devices: single crystals do not suit for this purpose because of their small size and their spurious phases and cracks. These prototypes have shown to be advantageous with respect to ones realised with the conventional technology and, especially in the microwave field, superconducting devices seem to be valid candidates for commercialisation. The quality of the superconducting samples must be examined by means of measurements which allow to get information on the performances at microwave frequencies of the future device. A measurement of the microwave performance of the samples is the surface resistance,  $R_s$ . The surface resistance furnishes the dissipation for Joule effect on the surface of the sample and on the RF performance of the substrate material. Possible causes of dissipation are: phonons generation due to surface irregularities; acoustic phonons generation due to the interaction of the electromagnetic radiation with the crystalline lattice; presence of normal areas or depressed superconductivity regions; trapped magnetic flux during the cool down and losses at the grain boundaries. Defects and inclusions deeply limit the device performances in the microwave field: they generate losses and, as a consequence, increase the surface resistance. This information is not present in DC because the first established percolative superconducting path causes the short-circuit of the whole sample [31].

At low temperature it is possible to define the residual resistance,  $R_{RES}$ , which is a measurement of the intrinsic defects of the sample [32,33]. The  $R_{RES}$  is technologically important because it is the smallest obtainable RF loss [2,34]. Its lowering allows a great reduction of cross sectional dimensions and a corresponding miniaturisation of the devices.

To control the RF performance of the samples we have set up an experimental apparatus to measure their surface resistance by the dielectric resonator method at 10 GHz in the  $TE_{011}$  mode: it has the advantage to determine the quality of sample of any shape at different points on it.

### 2. THE DIELECTRIC RESONATOR METHOD

As is well known a cavity is an enclosure, in which the following boundary conditions must be satisfied: the zeroing of the tangential component of the electric field on the surface of the perfectly conducting resonant walls and the zeroing of the tangential component of the magnetic

field on the perfectly magnetic resonant walls. Inside the cavity there are stationary configurations of electromagnetic fields, called modes. Each of them is associated to a different harmonic time dependence, whose oscillating frequency is called resonance frequency.

Certain modes have the property that high frequency current do not flow in the joints between materials, so the use of one of these modes avoids that possible cause of the variation of response. The  $TE_{011}$  mode is always chosen because it vanishes at the dielectric metal interfaces.

In 1939, Richmyer [8] showed that unmetallized dielectric objects can work as electrical resonators which he called dielectric resonators [9–12]. In a dielectric material, with complex permittivity  $\varepsilon = \varepsilon' - j\varepsilon''$  and conductivity  $\sigma$ , we can define the loss tangent  $\text{tg}\delta$  as:

$$\text{tg}\delta = \frac{\omega\varepsilon'' + \sigma}{\omega\varepsilon'}$$

it considers both the loss in the dielectric due to the em incident wave and the dissipation due to the finite conductivity of the material. At microwave frequencies it is always  $\omega\varepsilon'' \gg \sigma$ . A cylindrical sample of low-loss high- $\varepsilon_r$  dielectric placed between parallel conducting plates forms a microwave dielectric resonator. The  $Q$ -factor of a resonator is:

$$Q_0 = \frac{f_0}{\Delta f}$$

where  $f_0$  is the resonance frequency and  $\Delta f$  is the half power bandwidth. Usually the  $Q$ -factor of a dielectric resonator is higher than that of a metal-walled cavity, this is due to the small dielectric and wall losses in the resonator.

In the past, different configurations have been studied: the dielectric resonator in free-space and in contact with conducting walls, the last structure is called the dielectric post resonator [13]. In the first configuration the resonance frequency and, as a consequence the  $Q$  factor, is evaluated by approximated methods, as the magnetic wall method in which the dielectric cylinder is contained in a contiguous magnetic-wall waveguide [14]; thus the dielectric resonator problem is reduced to a straightforward waveguide problem. In the magnetic wall model, the cylindrical surface containing the circumference of the resonator is replaced with a fictitious open-circuit boundary, the magnetic wall. In the second configuration it is possible to evaluate exactly the resonance frequency.

The surface resistance of superconductors,  $R_S$ , can be measured by several cavity methods [16]: the whole cavity made of superconductors [17–20] and one end-plate or both of them substituted by the superconductor. In the case of one end-plate [21,22], exact equations are available to compute the resonance frequency and the  $Q$ -factor of the cavity, as a consequence the  $R_S$  is readily linked to the  $Q$ -factor of the cavity by the geometric factor  $\Gamma$  of the cavity itself, which is defined as  $R_S = \frac{\Gamma}{Q_0}$ . In this method, the sensitivity is limited only by the loss on the metal walls, its

disadvantage is that it needs a calibration procedure. In the cavity perturbation methods, the two situations, i.e. the cavity with and without the sample, must be very similar, it means that the measured sample must be little if compared with the cavity itself, as a consequence two numbers of the same order have to be substrated. Anyway perturbation methods can be very accurate.

The dielectric resonator can be used to evaluate the surface resistance of superconductors. The parallel plate resonator technique [23], which consists of a dielectric spacer placed between two parallel superconducting samples, is the most sensitive, but it requires a numerical procedure to compute the surface resistance; its main disadvantages are the uncertainty on the distance between the samples and that this configuration it is not suitable to measure samples with  $R_S > 1 \div 2 \text{ m}\Omega$ , moreover a round robin must be performed to evaluate the  $R_S$  of a single sample. In [24,25] an alternative method employing a sapphire resonator between two superconducting samples is reported, in this case there are exact formulas for the resonance frequency and the  $Q$ -factor, but again a round robin must be performed. The dielectric resonator technique is used by [26], the sapphire is placed on the sample and the  $R_S$  is measured at 18.7 GHz. They use the Itoh and Rudokas model [27] to compute the resonance frequency, this method is based on a technique [28] for analysing the propagation characteristics of a rectangular dielectric waveguide. An experimental method has been performed to determine  $\Gamma$  and the parasitic quality factor, which

include the losses not generated by the sample. This method needs a preliminary calibration procedure for the sample shape and for the parasitic loss.

We measure the surface resistance by the dielectric resonator method at 10 GHz in the  $TE_{011}$  mode (X-band). In the configuration in use the dielectric, the  $TiO_2$ , is placed on the surface of the superconducting sample. This structure is enclosed in a copper cavity, which works as magnetic shield to avoid radiation losses. The boundary conditions to be satisfied are the zeroing on the three magnetic walls of the dielectric of the tangential component of the magnetic field and the zeroing of the electric field on the electric wall: the electric wall is the superconductor itself when it is cooled down to the transition temperature  $T_c$ . This system does not have the sensitivity to measure the surface resistance of the superconductor in the normal state. Because the dielectric is a flat disk-shaped, the magnetic field is strongest on its axis and, at a sufficient distance from it, the field resembles that of an axial magnetic dipole. Outside the dielectric, the electric and magnetic field decay almost exponentially as Bessel function of the II kind,  $K_0(x)$  and  $K_1(x)$ . The rutile is an anisotropic dielectric, but even though the two transverse dielectric constants are equal, they are different from the longitudinal ( $x$ -axis) constant. Anyway in the TE-modes,  $E_z = 0$  holds, so the dielectric properties of the rutile pellet in the resonator are affected by only a single dielectric constant  $\epsilon_r$ .

This structure has some advantages over, for instance, a hollow metal resonator with the thin film as end plate:

- because the fields are strongly concentrated in the dielectric, with an exponential fall-off outside, the proportion of total loss that is due to the sample is much greater;
- because the stored energy is lower, the sensitivity of the bandwidth to the sample surface resistance and hence the accuracy of measurements are both much greater;
- the sample shape can be any with a limitation: the minimum circle that can be inscribed on the sample must have a diameter of 10 mm, this is because the vanishing wave outside the dielectric pellet has been considered in the model;
- we can measure the surface resistance on different point of the same sample;
- we point out that the  $TE_{011}$  mode in a dielectric resonator systems is not degenerated by any other modes (as the  $TM_{111}$  in the case of the cavity), so it is not necessary to use any mode traps in such systems, anyway because the dominant mode is the  $TE_{111}$ , care must be taken not to excite other modes;
- this technique does not rely upon any calibration with other samples, since its geometric factor  $\Gamma$  can be derived from the electromagnetic fields solutions.

From the measured  $Q$  ( $Q_L$ ), we calculate the intrinsic factor  $Q_0$  by the following relation:

$$Q_0 = \frac{Q_L}{1 - 10^{\frac{IL}{20}}}$$

where IL are the insertion losses in decibels, which are measured at the resonance frequency.

From the definition of  $Q$ , we can write:

$$Q = \frac{\omega_0 W}{P}$$

where  $W$  the averaged stored electromagnetic energy and  $P$  is the dissipated power. The dissipated power is the sum of several contributions: the dissipated power for Joule effect ( $P_j$ ) in the conducting walls; the radiating power ( $P_r$ ) and the power loss in the dielectric ( $P_d$ ). The measured  $Q$  can be written as:

$$\frac{1}{Q_L} = \frac{1}{Q_0} + \frac{1}{Q_{ex}} \quad (1)$$

where  $Q_{ex}$  is the effect of exterior sources of dissipation. We can now define the coupling parameter  $\beta$  as:

$$\beta = \frac{Q_0}{Q_{ex}}$$

The coupling parameter is a measure of the efficiency with which the energy stored in the cavity coupling system is coupled to the external load and dissipated there. Three cases are possible:

1. if  $\beta < 1$ , the cavity is undercoupled;
2. if  $\beta = 1$ , the cavity is critically coupled;
3. if  $\beta > 1$ , the cavity is overcoupled.

In practice, we can trace back from the  $Q_L$  to the  $Q_0$  if we are in the case in which  $Q_{ex} \gg Q_0$ , i.e. if the resonator is weakly coupled with the measurement circuit.

The system can be sketched around the resonance frequency as a series or parallel equivalent LCR circuit. Under this simplification, the  $Q_{ex}$  has two contributions: the power transmitted to the circuit under test,  $P_t(\omega_0)$ , and to the supplying circuit,  $P_r(\omega_0)$ . Following this,  $Q_{ex}$  is the parallel between  $Q_{c,in}$  (input coupling) and  $Q_{c,out}$  (output coupling) [29]:

$$\frac{1}{Q_{ex}} = \frac{1}{Q_{c,in}} + \frac{1}{Q_{c,out}} = \frac{P_r(\omega_0)}{\omega_0 W} + \frac{P_t(\omega_0)}{\omega_0 W}$$

The equation (1) can be written as:

$$\frac{1}{Q_L} = \frac{1}{Q_0} + \frac{1}{Q_{c,in}} + \frac{1}{Q_{c,out}}$$

Now we define the power transmission coefficient as the ratio between the transmitted and the incident power, it is expressed by the relation:

$$T(\omega)_{dB} = \frac{P_{tr}(\omega)}{P_i(\omega)_{dB}}$$

It is possible to demonstrate that [30]:

$$T(\omega)_{dB} = \frac{4}{\frac{Q_{c,in}Q_{c,out}}{1} + \left(\frac{\omega}{\omega_0} - \frac{\omega_0}{\omega}\right)^2} \text{dB}$$

In the resonance condition, where  $\omega = \omega_0$ , we can define the insertion loss, IL, as:

$$IL = \frac{1}{T(\omega_0)_{dB}} = \frac{1}{\frac{4}{Q_{c,in}Q_{c,out}}} \text{dB} = 10 \log \left( \frac{Q_{c,in}Q_{c,out}}{4Q_L^2} \right)$$

If we assume that the coupling is symmetric:

$$Q_{c,in} = Q_{c,out} = Q_c \quad (2)$$

we can define the insertion ratio:

$$r_V = 10^{\frac{IL}{20}}$$

We are experimentally allowed to consider the assumption (2), in fact if we measure both  $S_{12}$  and  $S_{21}$  we do not find any significant difference between them. Following this and keeping in mind that,

$$\frac{1}{Q_L} = \frac{1}{Q_0} + \frac{1}{Q_{ex}}$$

we have:

$$Q_0 = \frac{1}{\frac{1}{Q_L} - \frac{r_V}{Q_L}} = \frac{Q_L}{1 - r_V}$$

from which follows:

$$Q_0 = \frac{Q_L}{1 - 10^{\frac{IL}{20}}}$$

Even if it is always possible to get  $Q_0$  from the measured  $Q$ , in general we prefer to decouple the resonance circuit so that the condition  $Q_0 \cong Q_L$  be realised minimising  $r_V$ , i.e.  $T(\omega_0)$ . In fact if we write the error propagation law with  $r_V \rightarrow 0$ , we find that the error on  $Q_0$  tends to the one on  $Q_L$ . As a consequence, for resonators weakly coupled to the measurement circuit, the error in the determination of the intrinsic  $Q$  is coincident with the measured one. In the case of a superconducting sample, the insertion loss decreases with the temperature. In the temperature range of interest, while the coupling can be considered almost unvaried, the loaded  $Q$  strongly decreases with the temperature up to  $T_c$ . Because both the ohmic and the dielectric losses increase with the increase of the temperature, the  $Q_L$  and  $Q_0$  decrease and so the IL decreases. Anyway in our samples it is always verified the condition  $IL < -30$  dB at any temperature.

Now we correlate  $Q_L$ , and as a consequence  $Q_0$ , to the surface resistance  $R_S$  of the superconductors ( $R_{S1}$ ) by the following expression:

$$\frac{1}{Q_L} = B_1 R_{S1} + B_2 R_{S2} + B_3 R_{S3} + A \operatorname{tg} \delta + \frac{1}{Q_c} + \frac{1}{Q_R}$$

The coefficients  $A$ , i.e. the energy stored fraction in the dielectric pellet, and  $B_i$  can be calculated for any axis symmetric geometry with the help of the finite element method, in which also the vanishing wave outside the sample has been considered.  $B_1$  depends on the geometry of the dielectric resonator and increases with the ratio between the diameter and the height of the dielectric.  $B_2$  and  $B_3$  are the contributions of the copper plates to the surface resistance.  $Q_c$  corresponds to the coupling losses and can be calculated by the  $S_{11}$  and  $S_{22}$  parameters;  $Q_R$  corresponds to the radiation losses and can be neglected as soon as the distance between the plates is smaller than the half wavelength at the opening frequency, i.e. if we are under the cut-off condition. This equation is valid for any TE mode in axial symmetry.

### 3. EXPERIMENTAL SET-UP

We measure the temperature dependence of the  $Q$ -factor of the dielectric resonator at 10 GHz from 20 K up to the temperature of the superconducting transition as a function of the input power between  $-5$  and 20 dBm. We define the superconducting critical temperature,  $T_C$ , as the first temperature, during the cooling down, at which it is possible to measure the  $\Delta f$  of the  $TE_{011}$  mode at 10 GHz. Therefore we define the residual resistance,  $R_{RES}$ , as the value at which the derivative of the surface resistance is zero.

In Fig. 1 we present a cross section of the experimental apparatus. The excitation of the RF power is performed by two coupling belt loops placed in the upper plate of the cavity: we have experienced that their shape is unimportant, provided that they are in axis between them. The geometrical dimensions of the coupling are not small, if compared with the wavelength, so we speak of line coupling, which is a mixed coupling through the electric and the magnetic field. The  $TiO_2$  has a diameter of 7 mm with a height of 1 mm, its dielectric constant  $\epsilon_r$  is 90 at 77 K and the loss tangent is  $2 \times 10^{-5}$  in the temperature range of interest.

The measurements are performed by means of a Network Analyzer (NA) HP 5810B. The NA is connected to the cavity by cables, which losses are less than 0.5 dB between 8 and 12 GHz between 20 K and room temperature.

The cavity is mounted on a cold finger. The vacuum reached in the chamber ( $<10^{-4}$  atm) allows to have a temperature difference between the top and the bottom of the cavity below 1 K. The sample temperature is measured by a silicon diode thermometer placed inside the copper 2 mm under the its bottom.

The sintered pellets have been prepared by citrate pyrolysis samples; the films have been grown *in situ* by the 90° off-axis magnetron sputtering technique, their thickness ranges between 1000 and 6000 Å: the details about their preparation are described elsewhere [5,35].

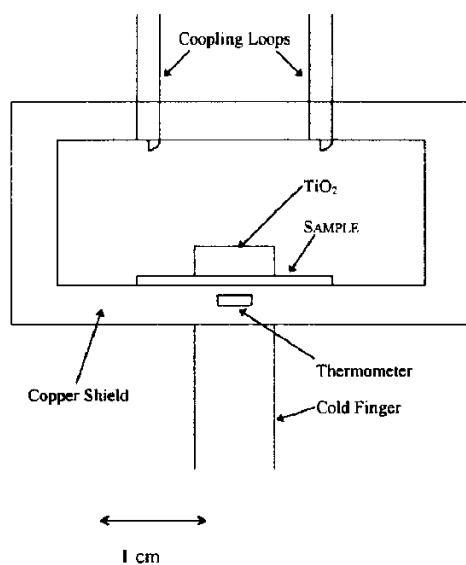


Fig. 1. Cross section of the resonant system for surface resistance measurements by the dielectric resonator method.

Because the surface resistance depends strongly on impurities on the surface, before every measurements the YBCO sample and the cavity are mechanically and chemically treated to remove pollution. After this, the sample is placed on the lower plate of the cavity, kept jointly with it by a low loss ( $<10^{-4}$ ) silicon paste. The rutile is placed in the same way on the sample and it is centred in the cavity with a tolerance less than 0.1 mm.

The data acquisition is computer-controlled by a HP system. For the  $S_{21}$  (or  $S_{12}$ ) parameter we calibrate the instruments by the through connection in the band in which the resonance peak shifts as the temperature increases between 20 and  $T_C$ . The acquisition program performs several zooms to have the peak at  $-3$  dB at full screen. We obtain, in this way, the maximum sensitivity possible. By this procedure the  $Q_L$  is measured without calibration: we have experienced that the difference between the measurement with and without the calibration is within the experimental sensitivity by this procedure.

The  $Q$  values range from 30 000 down to 100, which corresponds to a  $R_S$  equal to 0.7 and 627 m $\Omega$ , respectively: this method shows to have a high dynamic range (the  $R_S$  varies up to 3 decades). The performed measurements are characterised by an error within few percent, with a repeatability less than 1%.

#### 4. EXPERIMENTAL RESULTS

In Table 1 we show the results on the YBCO samples compared with a copper plate at an input power equal to 10 dBm. We want to remark that this work is not an exhaustive study on the effects of the sample thickness on the RF properties; in this connection further work is in progress.

Table 1

Sample id	Thickness	$R_{RES}$ (m $\Omega$ )	$T_C$ (K)	$R_S$ (at $T_C$ ) (m $\Omega$ )
FY1294	5000 Å	0.73	88.13	154.56
FY1394	3000 Å	1.36	89.09	64.39
FY0295	5000 Å	0.85	87.55	254.58
FY0495	5000 Å	0.71	89.67	627.18
FY1195	6000 Å	1.09	88.03	76.85
FY1995	1000 Å	1.06	86.54	54.61
FY0196	5000 Å	0.75	86.11	483.91
PBY0196	2 mm	16.22	90.06	570.04
PBY0296	2 mm	23.44	87.09	489.09
PBY0396	2 mm	26.03	85.55	367.24
Copper	2 mm	6.85	—	—

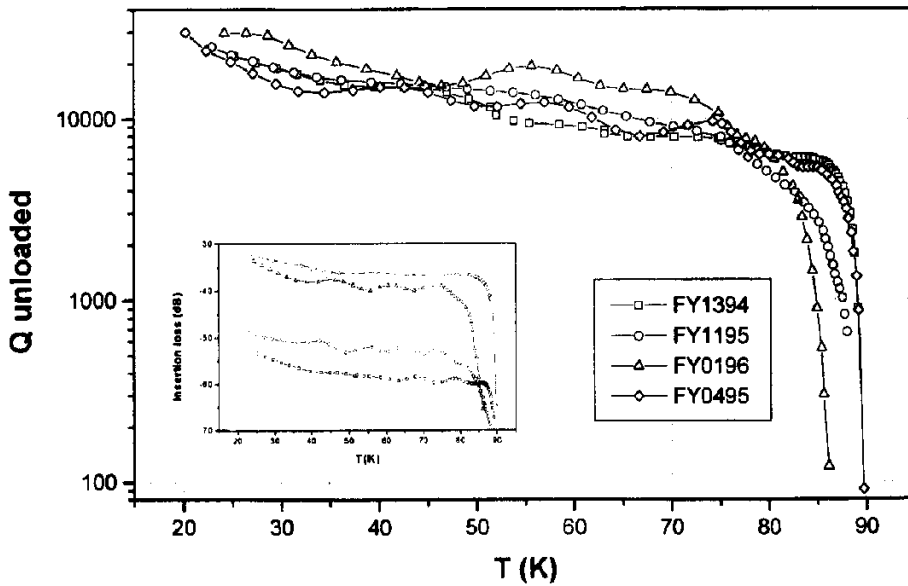


Fig. 2. Unloaded  $Q$ -factor measured as a function of the temperature for different samples. In the inset the outgoing of the insertion loss.

In Fig. 2 we show the unloaded  $Q$  measured as a function of the temperature. In the inset the insertion losses is shown. We can verify that the  $S_{21}$  parameter is always less than 30 dB, as a consequence the cavity is strongly undercoupled as previously explained.

In Fig. 3 we show the plot of the surface resistance, normalised to the  $R_S$  value measured at  $T_C$ , as a function of the reduced temperature. In the inset the measured  $R_S$  is presented as a function of the reduced temperature. We can notice the sharper transition of the 5000 Å samples. The derivative of  $R_S$  in FY1394 and FY1195 is higher with a higher residual resistance. The  $R_S(T_C)$  is higher in the samples with lower residual resistance. The FY1394 sample, measured more than 1 year after the deposition, shows a sharp transition and high  $T_C$ , but its residual resistance is not very good if compared with other samples. This could be due to a probable surface pollution during this time, even though the oxygen content is not significantly decreased.

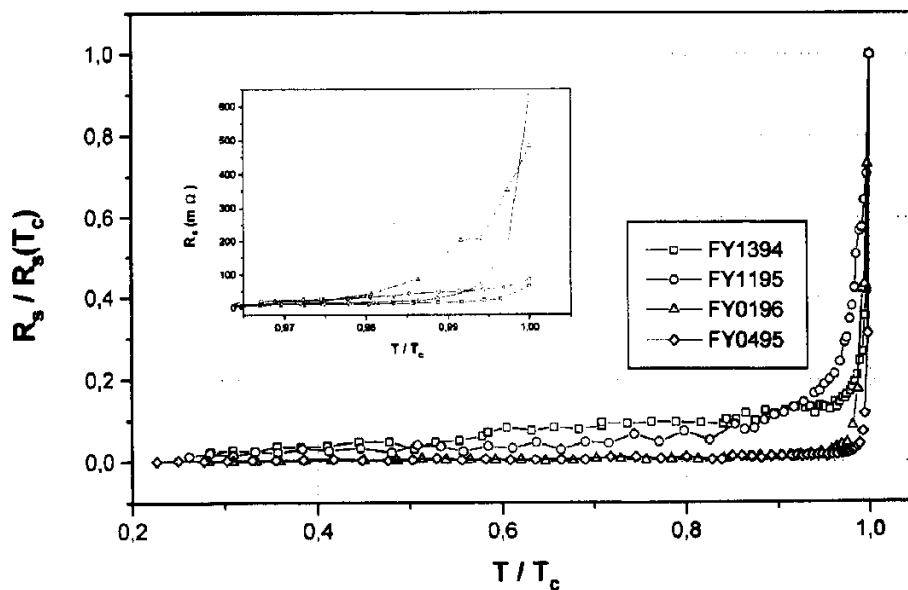


Fig. 3. Normalised surface resistance remased as a function of the reduced temperature for films. In the inset we show the  $R_S$  values near the transition.

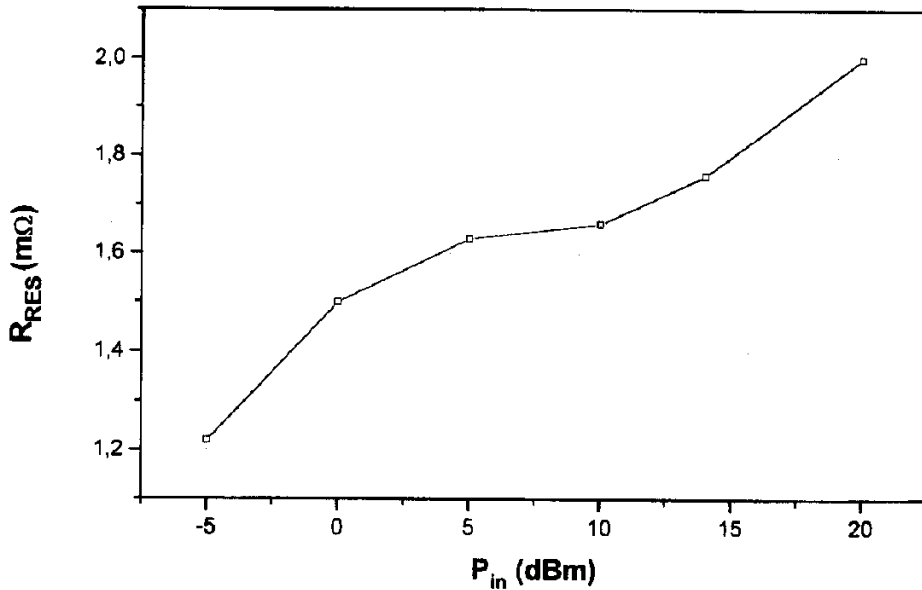


Fig. 4. Residual resistance measured as a function of the input power.

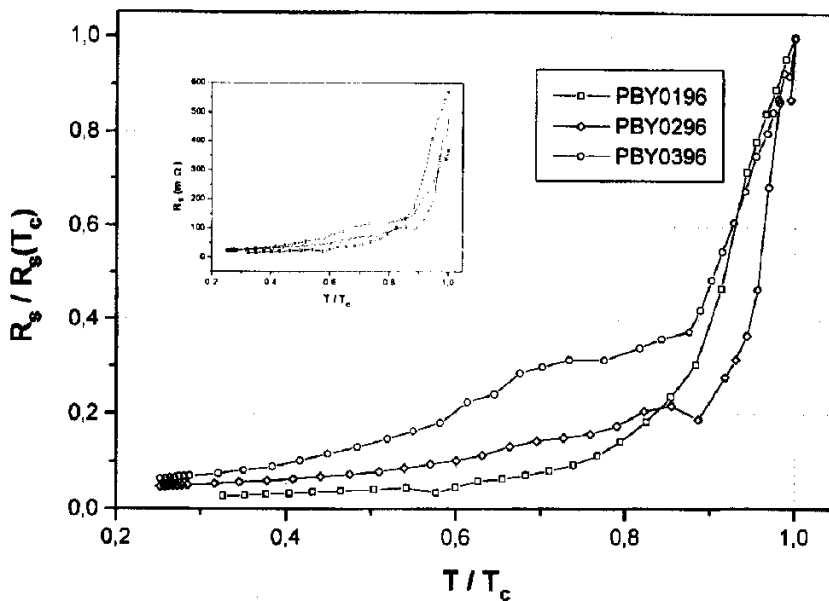


Fig. 5. Normalised surface resistance measured as a function of the reduced temperature for bulks. In the inset we show the  $R_s$  values.

In Fig. 4 we report the residual resistance as a function of the input power for a 5000 Å film (FY1396), showing that the input power increases the residual resistance, i.e. the losses.

In Fig. 5 we show the surface resistance of sintered samples, which results are summarised in Table 1.

## 5. CONCLUSIONS

We have set up an easy experimental apparatus for measurement of the surface resistance of superconducting samples at 10 GHz. The sample shape is unimportant, provided that the minimum circle inscribed on the sample surface is 10 mm. The sample measurement does not



need previous calibration on standard samples. This method shows a high dynamic range, in fact  $R_S$  varies up to 3 decades.

We can affirm that low residual resistance corresponds to an RF signal with high SNR and high critical temperature reflecting a high oxygen content. RF properties are optimised for sample thickness equal to 5000 Å, which seems to be promising for the realisation of superconducting devices.

#### REFERENCES

1. R. Weight, A. A. Valenzuela and P. Russer, *Appl. Supercond.*, **1**, 1595 (1993).
2. N. Newman and W. G. Lyons, *J. Supercond.*, **6**, 119 (1993).
3. E. Belohoubek, E. Denlinger, D. Kalokitis, A. Fathy, R. Paglione, V. Pendrik, J. Brown, A. Pique, X. D. Wu, S. M. Green, S. Mathews, R. Edwards, M. Mathur and T. Venkatesan, *J. Supercond.*, **5**, (1992).
4. E. Belohoubek, D. Kalokitis, A. Fathy, E. Denlinger, A. Pique, X. D. Wu, S. M. Green and T. Venkatesan, *Appl. Supercond.*, **1**, 1555 (1993).
5. N. Sparvieri, A. M. Fiorello, L. Marescialli and M. Ambrico, *Il Nuovo Cimento*, **16**, 2005 (1994).
6. J. van Bladel, *IEEE Trans. on Micr. Th. and Techn.*, vol. MTT-23, pp. 199–208, Feb. (1975).
7. M. Jawronski and M. W. Pospieszalski, *IEEE Transactions on Microwave Th. and Techn.*, vol. MTT-27, pp. 639–643, Jul. (1979).
8. R. D. Richmyer, *J. Appl. Phys.*, **10**, (1939).
9. J. K. Plourde and C. Ren, *IEEE Transactions on Microwave Th. and Techn.*, vol. MTT-29, pp. 754–770, Aug. (1981).
10. A. Okaya and L. F. Barash, *Proc. IRE*, vol. **50**, pp. 2081–2092, Oct. (1962).
11. Y. Konishi, N. Hoshino and Y. Utsumi, *IEEE Trans. in Micr. Th. and Techn.*, vol. MTT-24, pp. 112–114, Feb. (1976).
12. M. W. Pospieszalski, *IEEE Trans. on Micr. Th. and Techn.*, vol. MTT-27, pp. 233–238, Mar. (1977).
13. M. W. Pospieszalski *IEEE Trans. on Micr. Th. and Techn.*, vol. MTT-25, pp. 228–231, Mar. (1977).
14. S. B. Coh, *IEEE Trans. on Micr. Th. and Techn.*, vol. MTT-16, pp. 218–227, Apr. (1968).
15. P. Guillon and Y. Garault, *IEEE Trans. on Micr. Th. and Techn.*, vol. MTT-25, pp. 916–922, Nov. (1977).
16. A. M. Portis, D. W. Cooks and E. R. Grey, *J. Supercond.*, (1990).
17. H. Padamsee, J. Tuckmante and W. Weingarten, *IEEE Trans. on Magn.*, MAG-19, pp. 1308–1311, May (1983).
18. W. Bauer, S. Giordano and H. Hahn, *J. Appl. Phys.*, (1974).
19. T. W. Button and N. M. Alford, *Appl. Phys. Lett.*, **60**, 1378 (1992).
20. E. Minehara, R. Nagai and M. Takeuchi, *J.J.A.P.*, **28**, L100 (1989).
21. R. Fastampa, M. Giura, R. Marcon and E. Silva, *Meas. Sci. Technol.*, 1172 (1990).
22. N. Klein, G. Muller, S. Orbach, H. Piel, H. Chaloupka, B. Roas, L. Schultz, U. Klein, and M. Peiniger, *Phys. C*, **162–164**, 1549 (1989).
23. R. C. Taber, *Rev. Sci. Instrum.*, **61**, 2200 (1990).
24. C. Wilker, Z. Y. Shen, V. X. Nguyen and M. S. Brenner, *IEEE Trans. on Appl. Supercon.*, **3**, 1457 (1993).
25. J. Krupka, M. Klinger, M. Kuhn, A. Baranyak, M. Stiller, J. Hinken and J. Modelski, *IEEE Trans. on Appl. Supercon.*, **3**, 3043 (1993).
26. N. Klein, U. Dahne, U. Poppe, N. Tellmann, K. Urban, S. Orbach, S. Hensen, G. Muller and H. Piel, *J. Supercond.*, **5**, 195 (1992).
27. T. Itoh and R. S. Rudokas, *IEEE Trans. on Micr. Th. and Techn.*, MTT-25, pp. 52–56, Jan (1977).
28. E. A. J. Marcatili, *Bell Syst. Tech. J.*, **48**, 2071 (1969).
29. K. H. Young, G. V. Negrete, R. B. Hammond, A. Inam, R. Ramesh, D. L. Hart and Y. Yonezawa, *Appl. Phys. Lett.*, **58**, 1789 (1991).
30. M. Sucher and J. Fox, *Handbook of microwave measurements*, J. Wiley and Sons Inc., 1963, Third Edition, Vol. II, New York, London.
31. J. Halbritter, *Z. Phys.*, **266**, 209 (1974).
32. H. Pfister, *Cryogenics*, (1976).
33. A. M. Portis, *J. Supercon.*, **5**, 319 (1992).
34. D. E. Oates, P. P. Nguyen, G. Dresselhaus, M. S. Dresselhaus, G. Koren and E. Polturak, *J. Supercond.*, **8**, (1995).
35. N. Sparvieri, P. Cattarin, M. Boutet, B. Camorota, G. Russo and F. G. Ricciardiello, *Interceram, International Ceramic Review*, **44** 292 (1995).